Virology 531 (2019) 114–125

Contents lists available at ScienceDirect

Virology

journal homepage: www.elsevier.com/locate/virology

The BOLF1 gene is necessary for effective Epstein–Barr viral infectivity

H. M. Abdullah Al Masud[a], Takahiro Watanabe[a], Yoshitaka Sato[a], Fumi Goshima[a], Hiroshi Kimura[a], Takayuki Murata[a,b,*]

[a] Department of Virology, Nagoya University Graduate School of Medicine, Nagoya, Japan
[b] Department of Virology and Parasitology, Fujita Health University School of Medicine, Toyoake, Japan

ARTICLE INFO

Keywords:
EBV
BOLF1
BKRF4
Tegument
BAC
CRISPR/Cas9

ABSTRACT

The Epstein–Barr virus (EBV) is a causative agent of infectious mononucleosis and several malignancies. Here, we focused on an EBV lytic protein, BOLF1, which is conserved throughout the herpesvirus family and is reported to be a virion tegument protein. We first constructed BOLF1-deficient viruses using the bacterial artificial chromosome (BAC) and CRISPR/Cas9 systems. Although the loss of BOLF1 had almost no effect on viral protein expression, DNA synthesis, or extracellular progeny release, EBV infectivity was significantly reduced. Further analysis showed that nuclear transportation of the incoming virus was decreased by the disruption of BOLF1. Our results indicate that BOLF1enhances the infectious potential of progeny virions, at least partly by increasing nuclear transportation of incoming nucleocapsids. We also found that BOLF1 interacted with BKRF4, and the BOLF1 and BKRF4 proteins were localized in the nucleus and perinuclear area, during the viral lytic cycle.

1. Introduction

The Epstein–Barr virus (EBV) is a human gammaherpesvirus found in > 90% of the world's population. EBV infection occurs primarily during early childhood and is generally asymptomatic at that time. However, infection during adolescence or older is often associated with infectious mononucleosis. Upon infection, the EBV remains latent in the B cells and cannot be eradicated by the host immune system. A long-term EBV infection can cause several types of cancers, including Burkitt lymphoma, Hodgkin lymphoma, nasopharyngeal carcinoma, and gastric carcinoma (Young and Rickinson, 2004).

Although EBV maintains a latent infection in the host cells, it can occasionally switch from the latent to the lytic state. This phenomenon is termed reactivation. In the latent state, EBV DNA exists as episomes in the nuclei of infected cells (Lieberman, 2015; Murata et al., 2014). Due to chromatinization, the expression of EBV genes is limited. The number of EBV genes expressed in the latent state depends on the cell type and cellular milieu. For example, only the transcription of non-coding RNAs, EBV-encoded small RNAs (EBERs) has been detected in memory B cells. In EBV-positive gastric carcinomas, the EBV nuclear antigen (EBNA) 1 is produced in addition to EBERs. When primary B cells are infected with EBV in cell cultures, the resultant EBV-positive cells start to proliferate efficiently, which are called lymphoblastoid cell lines (LCLs). These LCLs produce EBERs, EBNA1, EBNA2, EBNA3A, EBNA3B, EBNA3C, EBNA-LP, latent membrane protein (LMP) 1, LMP2A, and LMP2B.

Upon reactivation, EBV expresses more than 80 genes, synthesizes viral genomic DNA, and eventually produces progeny viruses (Hammerschmidt and Sugden, 2013; Murata and Tsurumi, 2014). The causes of EBV lytic reactivation in vivo is not fully understood, but in cell cultures, several chemical and biological stimuli can initiate reactivation, including 12-O-tetradecanoylphorbol-13-acetate, histone deacetylase inhibitors, and transforming growth factor β. These stimuli induce transcription of the viral immediate–early genes BZLF1 (also known as Zta, ZEBRA or EB1) and BRLF1 (Rta). As transcriptional activators, these immediate–early genes can enhance the expression of early genes, which include those necessary for viral DNA genome replication, such as the single-stranded DNA-binding protein BALF2, viral DNA polymerase BALF5, and the EBV DNA polymerase processivity factor BMRF1. After viral DNA amplification in the replication compartments of the nucleus, viral late gene transcription occurs. Many of the late genes encode viral structural proteins, such as capsid proteins, tegument proteins, and glycoproteins. Viral genomic DNA amplified during the lytic cycle is incorporated into an assembled icosahedral capsid in the nucleus, where some of the tegument proteins may attach to the nucleocapsid. The nucleocapsid buds into the inner nuclear membrane, temporarily acquires an envelope (initial envelopment), and is excreted into the cytoplasm. The nucleocapsid then gains another envelope, presumably at the *trans*-Golgi network (secondary envelopment). At this step, other tegument proteins are also incorporated into

* Correspondence to: Department of Virology and Parasitology, Fujita Health University School of Medicine, Toyoake, Aichi 470-1192, Japan.
E-mail address: tmurata@fujita-hu.ac.jp (T. Murata).

https://doi.org/10.1016/j.virol.2019.02.015
Received 15 November 2018; Received in revised form 14 February 2019; Accepted 22 February 2019
Available online 23 February 2019
0042-6822/

the virion at the surface of the *trans*-Golgi network or other membranous organelles yet to be identified. Finally, the virion is secreted from the host cell. Because the EBV virion particle is enveloped, the viral genome in the particle is resistant to DNase. To infect another cell, the virion attaches to the cell surface via the CD21 protein and then is internalized into the cell and transported to the nucleus. The subsequent expression of viral genes in the nucleus indicates a successful infection cycle (Hammerschmidt and Sugden, 2013; Murata, 2014).

Although the EBV genes expressed during the latent stage have been evaluated extensively, the genes related to the lytic cycle, especially those encoding tegument proteins, remain relatively unknown. Currently, the tegument proteins of alphaherpesviruses, including the herpes simplex virus 1 (HSV-1) and the pseudorabies virus (PrV), are better understood than those of EBV. However, these proteins play critical roles in envelopment, virion morphogenesis, intracellular transportation, and efficient infection (Diefenbach, 2015; Owen et al., 2015; Sathish et al., 2012), and information on tegument proteins and their functions will contribute greatly to more thorough understanding of the molecular mechanism of the lytic replication cycle of EBV. EBV tegument proteins are difficult to research because mutagenesis of the EBV genome is challenging. In addition, lytic replication of EBV is not as efficient as that of HSV-1 or PrV. To address these challenges, we developed two techniques for mutagenesis of the EBV genome: the BAC and CRISPR/Cas9 systems. Using these techniques, we were able to analyze the role of an EBV gene, BOLF1, in this study.

EBV BOLF1 encodes a tegument protein (Johannsen et al., 2004) of 1239 amino acid residues and is conserved among all members of the herpesvirus subfamily. Because BOLF1 associates with BPLF1, also known as the large tegument protein, BOLF1 is also called the large tegument protein-binding protein (Murata, 2018). Whereas the functions of BOLF1 homologs in alphaherpesviruses have been investigated extensively, the physiological roles of EBV BOLF1 have not been reported.

In HSV-1, UL37, the homolog of BOLF1, has been shown to be important for egress and secondary envelopment, as the release of infectious virions is prevented in UL37-deficient HSV-1, with unenveloped progeny capsids accumulating in the cytoplasm (Desai et al., 2001; Klupp et al., 2001; Leege et al., 2009). PrV UL37 is reported to have similar characteristics to those of HSV-1 UL37 (Leege et al., 2009). UL37 of HSV-1 and PrV must interact with UL36, the homolog of BPLF1 (Klupp et al., 2002; Vittone et al., 2005), for efficient secondary envelopment (Desai et al., 2008; Kelly et al., 2014). HSV-1 UL37 also interacts with viral membrane proteins, such as glycoprotein K and UL20, while UL36 binds to the capsid vertices (Cardone et al., 2012). Thus, the interactions among membrane proteins, UL37, UL36, and the capsid lead to efficient envelopment of the HSV. Additionally, UL37 is involved in both retrograde and anterograde transport along the microtubules during ingress and egress (Pasdeloup et al., 2013; Richards et al., 2017). Recently, it was shown that HSV-1 UL37 downregulated innate immune activation via deamidation of cyclic GMP–AMP synthase in mice and humans (Zhang et al., 2018).

Deletion of the UL47 gene, the human cytomegalovirus (HCMV) homolog of EBV BOLF1, in betaherpesvirus lowered the progeny titer approximately 100-fold, and the mutant appeared to be less infectious than the wild-type (Bechtel and Shenk, 2002). Cytoplasmic accumulation of non-enveloped capsids, as well as inefficient linkage between tegument proteins and capsids, was observed in cells infected with the UL47 knockout virus (Cappadona et al., 2015). A process after entry and before immediate–early gene expression was also inhibited by the loss of UL47 (Bechtel and Shenk, 2002). Like other BOLF1 homologs, UL47 interacts with UL48, a homolog of BPLF1 (Tullman et al., 2014).

In a mutagenesis experiment using the murine gammaherpesvirus 68, the ORF63 gene (a homolog of BOLF1) appeared to have an essential function (Song et al., 2005). The deletion of ORF63 in murine gammaherpesvirus 68 caused a severe growth defect and inhibited nuclear transportation of incoming nucleocapsids (Latif et al., 2015). An ORF63-knockout mutant of Kaposi sarcoma-associated herpesvirus (KSHV) has not been created yet, but the interaction between ORF63 and ORF64 (homolog of BPLF1) has already been elucidated (Rozen et al., 2008). Similar to HSV-1 UL37, KSHV ORF63 helps the virus evade host innate immunity by inhibiting nucleotide binding, oligomerization, and the leucine-rich repeat-mediated innate immune response (Gregory et al., 2011).

Because EBV BOLF1 has low amino-acid similarity to its homologs in other herpesviruses, it may have different functions from its homologs. To investigate these functions, we constructed BOLF1-deficient viruses using the BAC system and found that the loss of BOLF1 had almost no effect on the production of viral proteins, DNA replication, or extracellular progeny secretion, but it significantly reduced *de novo* infectivity. Nuclear transportation of the incoming nucleocapsid was decreased, while attachment of the progeny virus was not affected by mutation of the BOLF1 gene. Similar results were obtained when BOLF1 knockout was generated by the CRISPR/Cas9 system using different EBV strains. Further, we observed that BOLF1 interacted with another EBV tegument protein, BKRF4, and the subcellular localization of BOLF1 was altered when it was co-expressed with BKRF4. Taken together, the importance of BOLF1 in the EBV lytic cycle was demonstrated.

2. Results

2.1. Construction of a BOLF1-deficient EBV-BAC strain

To investigate the functions of BOLF1 in the EBV lytic life cycle, we constructed a BOLF1-deficient recombinant EBV using the EBV-BAC system (Fig. 1A). We first generated an intermediate strain by inserting the Neo/St cassette into the wild-type EBV-BAC (B95-8). A dBOLF1-stop mutant was prepared by swapping the Neo/St cassette with the BOLF1 sequence containing a stop codon (T_{172}TT to TAA). Then the Neo/St cassette was inserted again and substituted with the BOLF1 wild-type sequence to generate a revertant virus (dBOLF1-stop/R) from the dBOLF1-stop mutant. To check the integrity of the viral genome, EBV-BAC DNA was digested using the *Bam*HI or *Eco*RI restriction enzymes, and the digested products were examined by electrophoresis (Fig. 1B). The band patterns of the three strains (wild-type, dBOLF1-stop, and dBOLF1-stop/R) were identical, indicating that the recombinant viral genomes did not have obvious deletions or insertions (Fig. 1B). We also confirmed that the intended mutation was introduced in the dBOLF1-stop mutant and corrected in the dBOLF1-stop/R mutant (unpublished data). The EBV-BAC DNA was transfected into HEK293 cells by lipofection and selected using hygromycin. We then cloned the green fluorescent protein (GFP)-positive, hygromycin-resistant colonies, in which the recombinant EBV genome was latently maintained.

2.2. Loss of BOLF1 decreased EBV infectivity

After transfecting the HEK293 cells, which maintained the latent recombinant EBV genomes (wild-type, dBOLF1-stop, and dBOLF1-stop/R), the cells were further transfected with an expression vector encoding BZLF1. Because BZLF1 encodes a viral transcription factor that can act as a reactivation switch, the EBV lytic stage is reactivated in the cells after BZLF1 transfection.

We used immunoblotting to examine if other viral lytic genes were expressed in the BOLF1 knockout strain (Fig. 2A). BZLF1 protein was expressed 2 days after transfection in either of the cell clones. We then measured viral lytic gene expression with early (BALF2, BMRF1, and BALF5) and late (BKRF4, BRRF2, and BALF4(gB)) kinetics, as well as the latent protein EBNA1. All proteins were expressed at similar levels in the wild-type, knockout, and revertant clones (Fig. 2A). A BOLF1 antibody was initially prepared to confirm the absence of the BOLF1 protein in the knockout virus, but this antibody did not detect the BOLF1 protein even in the wild-type and revertant samples due to

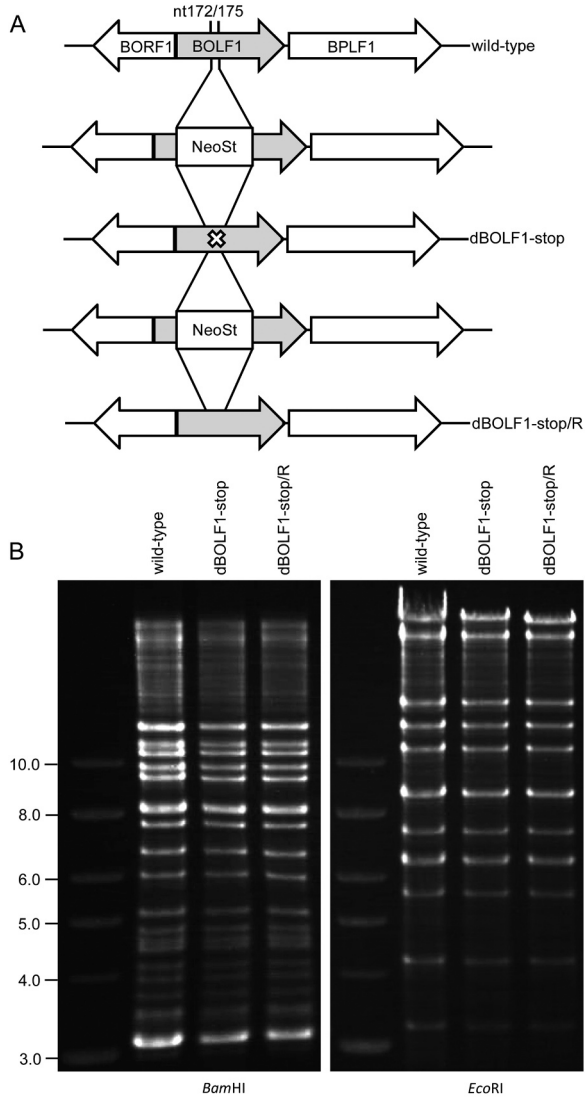

Fig. 1. BOLF1-deficient EBV mutant and revertant viruses were constructed using the EBV-BAC system. A) Diagrammatic representation of EBV-BAC recombination in *Escherichia coli*. The Neo/St cassette, which contains genes conferring neomycin resistance and streptomycin sensitivity, was inserted between nucleotides 172 and 175 of the BOLF1 gene. Next, the cassette was replaced by the BOLF1 sequence with a stop codon (T_{172}TT to TAA) to construct a BOLF1-deficient mutant (dBOLF1-stop). The Neo/St cassette was inserted into dBOLF1-stop and replaced with wild-type BOLF1 to construct the revertant virus (dBOLF1-stop/R). B) EBV-BAC DNA was digested by *Bam*HI and *Eco*RI, and the digested DNA was examined by agarose gel electrophoresis.

unknown reasons (unpublished data).

The levels of viral genomic DNA were also analyzed in the same cell lines. Background viral genomic DNA levels were similar among the wild-type, knockout, and revertant samples (Fig. 2B, black bars). Two days after transfection, replication of viral DNA in the knockout mutant occurred as efficiently as in the wild-type and revertant viruses (Fig. 2B, gray bars).

Lytic induction by BZLF1 transfection in EBV-positive HEK293 cells eventually results in the release of viral progeny into the culture medium. We measured viral DNA levels in the media using quantitative PCR (qPCR) (Fig. 2C). To eliminate from our measurements any naked DNA that was not packaged into virions, the media were sampled 3 days after BZLF1 transfection and treated with DNase, after which DNA was extracted and quantified. The levels of progeny release into the medium by the dBOLF1-stop mutant were comparable to those by the wild-type and dBOLF1-stop/R strains (Fig. 2C).

Next, The culture media were used to infect Akata(−) cells to determine if the DNase-resistant dBOLF1-stop particles (Fig. 2C) were indeed infectious. Because the recombinant EBV-BAC viruses express GFP, the infected cells became GFP positive. The loss of BOLF1 in the dBOLF1-stop mutant significantly decreased infectivity compared with the wild-type and revertant viruses (Fig. 2D).

After having the infectivity data above (Fig. 2D), we encountered a question, why infectivity reduced in the knockout viruses while there was no change in virus production (Fig. 2C). To address this question, we performed the binding assay and examined if attachment of the mutant virions to cells could be impaired. Akata(−) cells were inoculated with virus stocks for 3 h at 4 °C, followed by DNase treatment and extensive washing. Cell-associated viral DNA levels were then quantified by qPCR. In fact, the levels of the attached virion DNA were almost equal in the wild-type, mutant, and the revertant viruses (Fig. 2E).

We then asked if transportation of viral nucleocapsids to the nucleus was affected by the BOLF1 mutation. To this end, Akata(−) cells were infected with the recombinant viruses 3 h at 4 °C, followed by DNase treatment and extensive washing. Then the temperature was shifted to 37 °C and incubated for additional 6 h. Nuclei of the cells were isolated and subjected to DNA extraction and qPCR. As shown in the Table 1, when compared to the attached viral DNA levels, viral DNA transported into the nuclear fraction after the 6 h incubation period was markedly lower in the case of dBOLF1-stop (2.4%) rather than that of the wild-type (10.5%) and revertant (8.1%) viruses.

Overall, our data suggest that in HEK293 cells, disrupting BOLF1 had almost no effect on viral protein expression, DNA synthesis, or progeny release into the culture medium, but it significantly decreased the rate of infection to Akata cells. Attachment of the knockout virus to Akata(−) cells was not influenced, but nuclear transportation in Akata (−) cells was notably decreased by the disruption of BOLF1.

2.3. Successful trans-complementation of reduced infectivity in BOLF1-knockout virus

Our results indicate that BOLF1 helps increase the infectivity of viral progeny (Fig. 2). However, it was still possible that the reduced progeny infectivity of the knockout strain was attributed to a mutation outside of the BOLF1 gene. To confirm that the reduced progeny infectivity was indeed attributed to BOLF1 knockout, we conducted a *trans*-complementation assay (Fig. 3). HEK293 EBV-BAC cell clones were transfected with the BZLF1 expression vector with or without the BOLF1 expression vector (Fig. 3A). Three days after transfection, the supernatant was collected and analyzed to measure the infectious progeny titer as described for Fig. 2D. The BOLF1 knockout mutant without exogenous BOLF1 expression exhibited a decreased progeny titer, whereas BOLF1 co-expression successfully restored the level of infectivity (Fig. 3A). The infectivity of the wild-type and revertant strains was not markedly affected by exogenous expression of BOLF1 (Fig. 3A).

Cell proteins were sampled 2 days after transfection with the BZLF1 expression vector and subjected to immunoblotting (Fig. 3A). BOLF1 was not detected using an anti-HA antibody in the pcDNA + BZLF1-transfected cells but was detected in the BOLF1-HA + BZLF1-transfected cells (Fig. 3B). Similar levels of viral lytic proteins (BRLF1, BALF2, BMRF1, BALF4(gB), and BKRF4) were expressed in the knockout, wild-type, and revertant viruses (Fig. 3B). These results indicate that the disruption of BOLF1, but not an unrelated mutation, is responsible for the decreased infectivity of progeny virions produced using HEK293 cells.

2.4. BOLF1 deficiency created by the CRISPR/Cas9 system in Akata cells decreased viral infectivity

Analyses using the EBV-BAC B95-8 strain in HEK293 cells showed

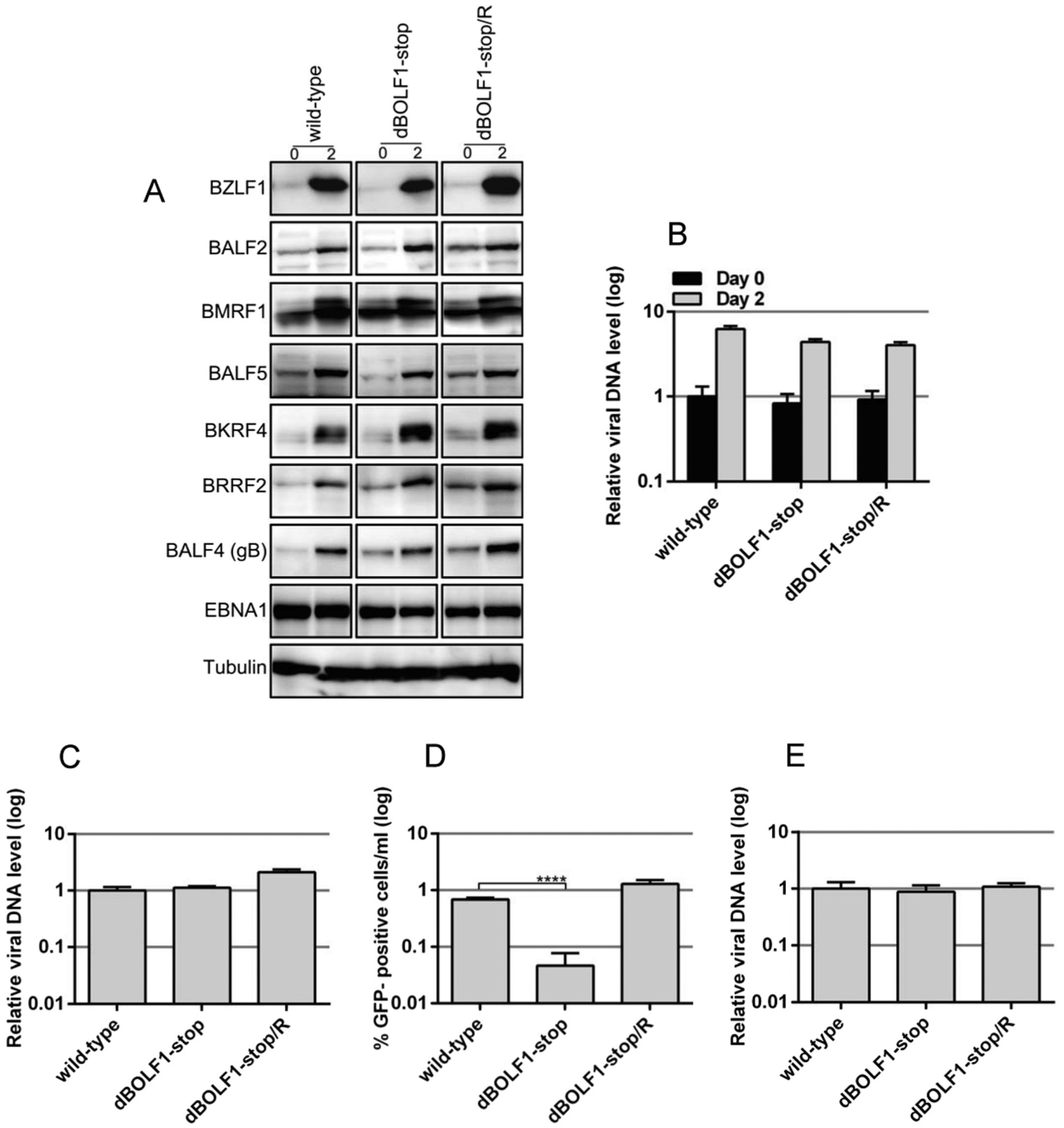

Fig. 2. Loss of BOLF1 significantly decreased *de novo* infectivity. Recombinant EBV-BAC DNA (described in Fig. 1) was transfected into HEK293 cells, and hygromycin-resistant, GFP-positive cell clones were isolated. A) Viral protein expression in the knockout EBV-BAC cells. The lytic cycle was induced by transfecting the BZLF1 expression vector into cell clones harboring latent EBV-BAC DNA. Cells were harvested immediately and at 2 days after transfection and subjected to immunoblotting. B) Viral DNA synthesis in the knockout EBV-BAC cells. Transfected cell clones were subjected to qPCR to detect the EBV DNA and genomic DNA in the host cells. Each bar represents the mean ± SD viral DNA level of three independent experiments (3 independent wells but experiments were performed simultaneously) after normalizing to the host genome DNA level. C) Production of DNase-resistant viral DNA from the knockout EBV-BAC cells. Three days after transfection, cell-free supernatant containing EBV particles were collected and digested with Turbo DNase I, followed by DNA extraction. Levels of viral DNA were quantified by qPCR. Each bar represents the mean ± SD DNA level of three independent experiments. D) Infectivity of EBV particles. The same supernatant containing viral particles from Fig. 2C was used to infect Akata(−) cells. After 2 days, GFP-positivity was determined by FACS analysis. Each bar represents the mean ± SD infectivity of three independent experiments. **** $p < 0.0001$, Student's *t*-test. E) Virion binding assay. The viral stock solutions were prepared as Fig. 2C and inoculated with Akata(−) cells at 4 °C with rotation for 3 h. The levels of virion DNAs attached to the host cells were quantified by qPCR.

Table 1
Nucelar transportation of EBV produced from HEK293.

	Nucleus-associated virus DNA/cell-attached viral DNA (%)
Wild-type	10.5
dBOLF1-stop	2.4
dBOLF1-stop/R	8.1

that BOLF1 is important for increasing viral infectivity. Next, we generated another strain of BOLF1-knockout EBVs, the Akata strain, and assessed the knockout effect in B cells (Akata cells), as B cell is the natural host of EBV. The mutation was introduced into BOLF1 by transfecting the CRISPR/Cas9 vector into AGS/EGFP–EBV cells, which maintain a recombinant Akata strain of EBV carrying EGFP and G418-resistance genes. Both mutated and non-mutated EBV strains were harvested from the transfected AGS/EGFP–EBV cell medium and used to infect Akata(−) cells. Cell clones were then selected using G418. Thus, we successfully isolated an Akata cell line that is latently infected with a BOLF1-deficient virus (BOLF1-knockout). Sequencing of the BOLF1-knockout viral genome confirmed a frameshift mutation in BOLF1.

After lytic induction using anti-IgG, we examined EBV gene expression (Fig. 4A), DNA synthesis (Fig. 4B), progeny production (Fig. 4C), and progeny infectivity (Fig. 4D). Protein samples were collected immediately and at 2 days after lytic induction and subjected to immunoblotting. Although we were not able to detect BOLF1 protein expression in all HEK293 cells, it was detected this time in the wild-type cells, but not in the Akata BOLF1-knockout cells (Fig. 4A, right panel). The expression levels of other viral proteins were similar between the knockout and wild-type viruses (Fig. 4A, left panel). The level of viral DNA synthesis was also similar between the knockout and wild-type viruses after lytic induction (Fig. 4B).

The disruption of BOLF1 gene in the Akata strain did not influence the secretion of DNase-resistant viral genomes into the culture medium (Fig. 4C), as observed in HEK293 cells (Fig. 2C). Progeny infectivity in the culture medium of infected Akata(−) cells was measured using fluorescence-activated cell sorting (FACS). While the level of DNase-resistant viral genomes was similar between the knockout and wild-type strains after IgG induction (Fig. 4C), infectivity of the knockout viruses was lower than that of the wild-type viruses by more than one order of magnitude (Fig. 4D). Binding ability of the knockout virus to Akata(−) cells was almost equal to that of the wild-type (Fig. 4E), but nuclear transportation of the nucleocapsid was decreased in the knockout strain (Table 2). These results indicate that loss of BOLF1 in viruses infecting Akata cells had little or no effect on viral protein expression, DNA synthesis, or progeny secretion. Attachment of the knockout virus to cells was normal, but nuclear transportation of the nucleocapsid was somehow decreased.

2.5. Interaction of BOLF1 with the BKRF4 protein

The herpesvirus virion structure is organized by multiple protein–-protein interactions (Diefenbach, 2015; Owen et al., 2015; Sathish et al., 2012). As ORF63, the BOLF1 homolog in KSHV, interacts with

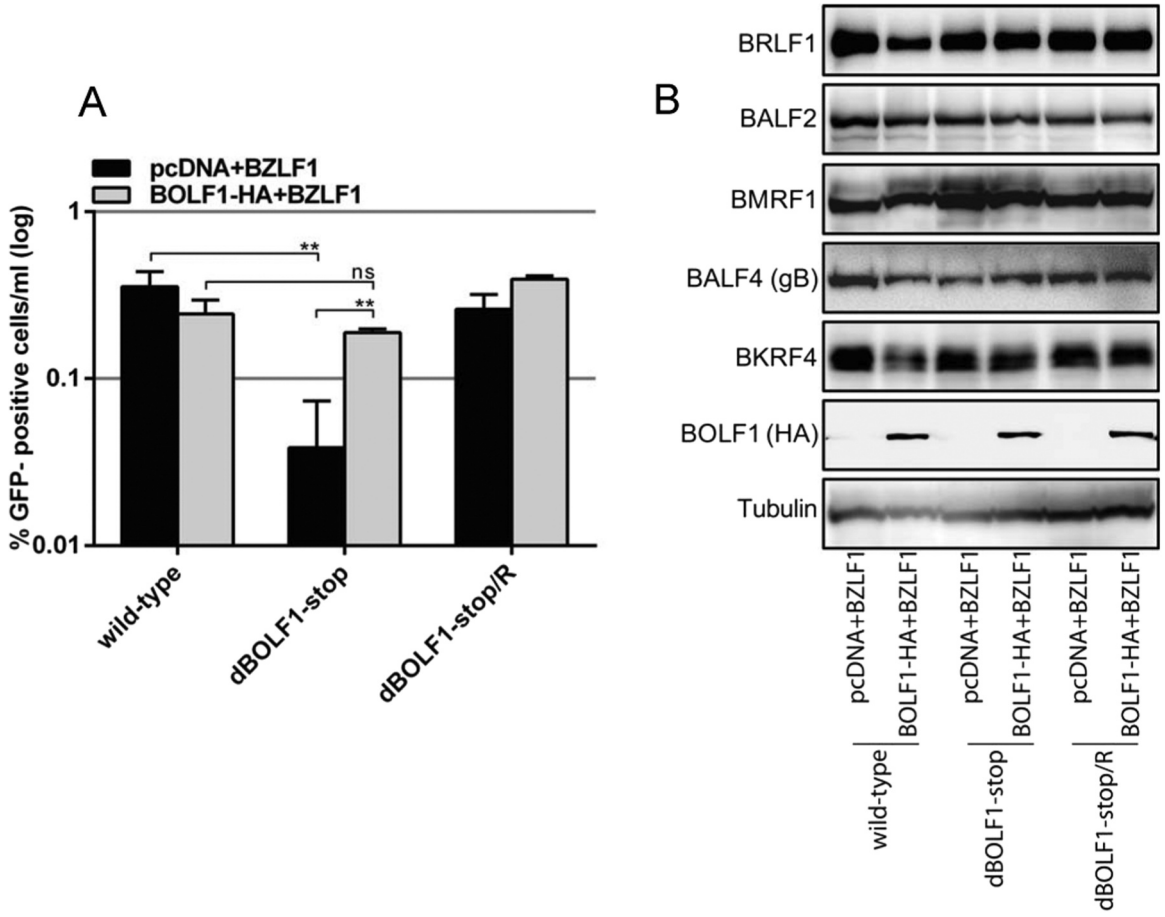

Fig. 3. Exogenous expression of wild-type BOLF1 successfully *trans*-complemented the impaired progeny titer of the knockout virus. A) HEK293 cell clones harboring latent EBV-BAC DNA (wild-type, dBOLF1-stop, and dBOLF1-stop/R) were transfected with indicated vectors. Three days after transfection, cell-free supernatants containing EBV viral particles were processed to determine the viral titer as described for Fig. 2D. Each bar represents the mean ± SD titer of three independent experiments. ** $p < 0.005$ and ns = not significant, Student's *t*-test. B) Transfected cells were harvested 2 days post-transfection and subjected to immunoblotting.

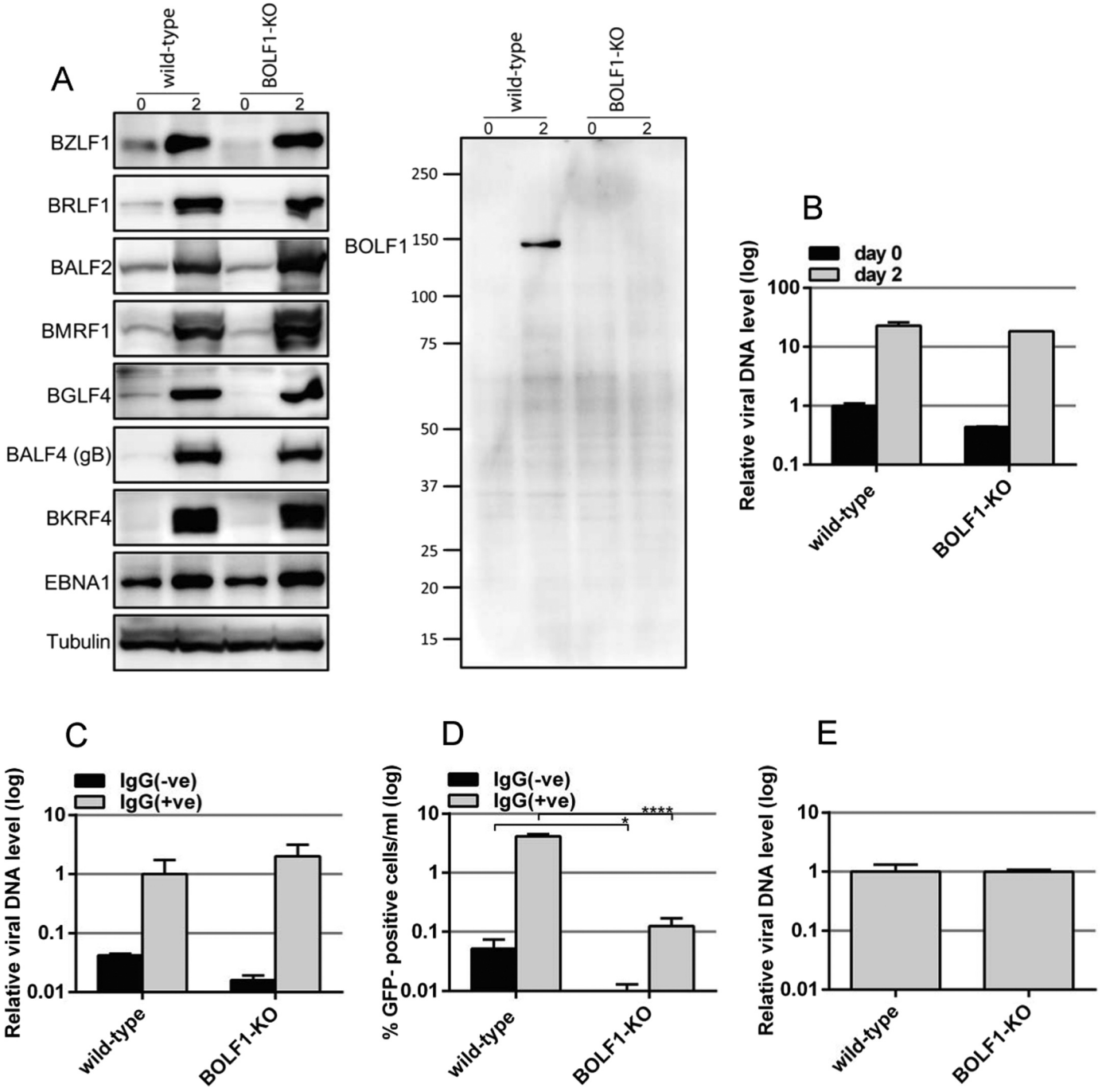

Fig. 4. BOLF1 disruption using the CRISPR/Cas9 system in Akata viruses reduced the efficiency of *de novo* infection. Using the CRISPR/Cas9 system, BOLF1 expression in the Akata virus was disrupted in AGS/EGFP–EBV cells. The viruses were used to infect Akata(−) cells, which were then cloned. Cell lines harboring the latent wild-type or BOLF1-knockout (BOLF1-KO) viruses were used in the following analyses. A) Viral protein expression in Akata cells infected with the BOLF1-KO Akata virus. For lytic induction, Akata cell clones (wild-type and BOLF1-KO) were treated with anti-IgG antibody for 0 or 2 days. Cells were then harvested and subjected to immunoblotting. B) Viral DNA synthesis in Akata cells infected with the BOLF1-KO Akata virus. Akata cell clones were treated with anti-IgG antibody and harvested immediately and at 2 days. The resulting viral DNA was subjected to qPCR as described for Fig. 2B. C) Production of DNase-resistant viral DNA from Akata cells infected with the BOLF1-KO Akata virus. Akata cell clones were treated with or without anti-IgG antibody for 2 days. Cell-free supernatants were collected and digested with Turbo DNase I, followed by DNA extraction. Viral DNA levels were quantified by qPCR. D) Infectivity of EBV particles. The same supernatants prepared in Fig. 4C were used to infect Akata(−) cells. After 2 days, GFP positivity was determined by FACS analysis. Each bar represents the mean ± SD infectivity of three independent experiments. * $p < 0.05$ and **** $p < 0.0001$, Student's *t*-test. E) Virion binding assay. The viral stock solutions were prepared as Fig. 4C and inoculated with Akata(−) cells at 4 °C with rotation for 3 h. The levels of virion DNAs attached to the host cells were quantified by qPCR.

ORF45, the homolog of the EBV tegument protein BKRF4 (Rozen et al., 2008), we investigated whether BOLF1 interacts with BKRF4. HEK293T cells were co-transfected with BOLF1 and BKRF4 expression vectors and subjected to immunoprecipitation assays using anti-HA antibodies, followed by immunoblotting (Fig. 5A). Similar to the KSHV homolog, FLAG-BRKF4 was co-precipitated with wild-type HA-BOLF1 (Fig. 5A). The binding was further confirmed by immunoprecipitation using anti-FLAG antibody (Fig. 5B).

Table 2
Nucelar transportation of EBV produced from Akata.

	Nucleus-associated virus DNA/cell-attached viral DNA (%)
Wild-type	12.6
BOLF1-KO	6.5

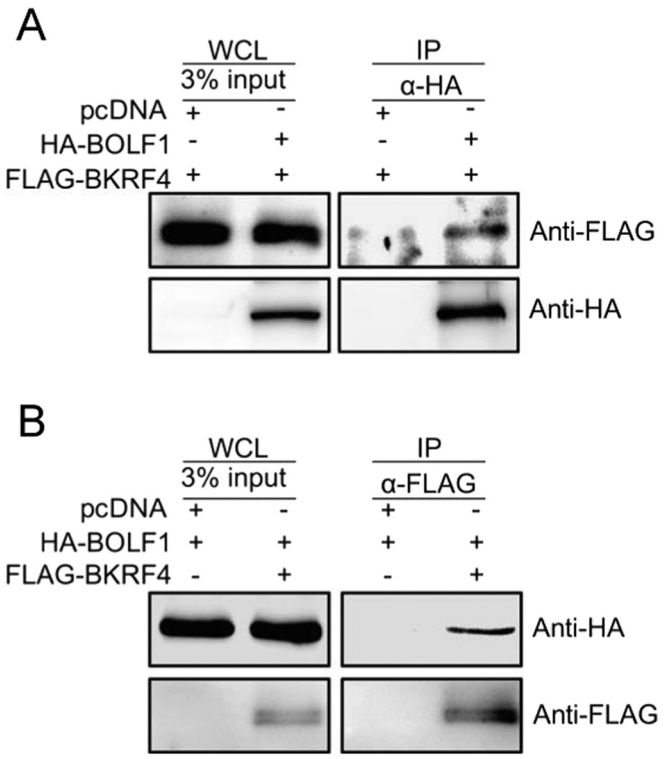

Fig. 5. BOLF1 interacted with BKRF4, another EBV tegument protein. (A, B) HEK293T cells were co-transfected with BOLF1 and BKRF4 expression vectors. Twenty-four hours after transfection, whole-cell lysates were collected and subjected to immunoblotting (left panels). The lysates were also subjected to immunoprecipitation using anti-HA (Fig. 5A) or anti-FLAG (Fig. 5B) antibody, followed by immunoblotting (right panels).

2.6. Subcellular localization of the BOLF1 protein in both transfected and infected conditions

The intracellular localization of the BOLF1 protein was determined by immunofluorescence analysis. Transfection of the BOLF1 vector alone into HeLa cells typically resulted in both nuclear and cytoplasmic localization, with more intense staining at the perinuclear region (Fig. 6, pcDNA + BOLF1-HA). This nuclear/cytoplasmic pattern was observed in 95% of expressing cells, while in rest of the cells, BOLF1 exhibited nuclear predominant localization (n = 39). As we reported in an earlier study (Masud et al., 2017), BKRF4 was detected predominantly in the nucleus and perinuclear region (Fig. 6, pcDNA + Flag-BKRF4). When the BOLF1 vector was co-transfected with the BKRF4 vector, the localization of BOLF1 was restricted to the nucleus only (Fig. 6, BOLF1-HA + Flag-BKRF4) (this nuclear staining pattern was seen in almost 100% of cells expressing both BKRF4 and BOLF1 (n = 30)), confirming the immunoprecipitation data that BOLF1 associates with BKRF4 (Fig. 5).

Next, the intracellular localization of the endogenous BOLF1 protein produced by lytic stage viruses was evaluated by immunofluorescence. The lytic cycle of AGS/EGFP–EBV cells was induced by BZLF1 transfection. Lytic induction was monitored by immunostaining of the EBV early protein BMRF1. In induced cells, BMRF1 was localized in the typical replication compartments in the nucleus (Daikoku et al., 2005), while BOLF1 was localized in the nucleus and perinuclear area (Fig. 7).

Finally, to further clarify the above-mentioned fact in the lytic stage, we analyzed localization of the endogenous BOLF1 and BKRF4 in the EBV-positive B cells (Akata cells). Akata wild-type, BKRF4-KO (Masud et al., 2017), and BOLF1-KO (prepared in Fig. 4) cells were lytically induced by anti-IgG treatment and subjected to the immunofluorescence analysis. In the wild-type cells, co-staining of the BOLF1 and BKRF4 showed that both the proteins localized in the nucleus and peri-nuclear area and partially co-localized in the nucleus (Fig. 8A). However, disruption of the BKRF4 gene had little or no effect on the localization pattern of BOLF1 (Fig. 8B). In the overexpression experiment, BKRF4 was needed for nuclear localization of BOLF1 (Fig. 6), but in the context of virus infection, it seems presence of BKRF4 was not required (Fig. 8B), possibly because another viral protein might alternatively retain BOLF1 in the nucleus. On the other hand, lack of BOLF1 also did not influence the nuclear localization pattern of BKRF4 (Fig. 8C).

3. Discussion

Homologs of EBV BOLF1 are present in all members of the herpesvirus family, and the α-helical secondary structures among the homologs are very similar, raising the possibilities that identical or similar functions are shared by the homologs. Nevertheless, homologies of amino acid sequences between the homologs are very low (15% or less, on average) (Latif et al., 2015; Russo et al., 1996). Indeed, the homolog proteins share only 8 amino acid residues conserved across the species despite the fact that they are all very large proteins (eg, BOLF1 of B95-8 strain EBV is consisted of 1239 amino acid residues). Therefore, whereas the functions of UL37 of alphaherpesviruses or other homologs have been well studied, the functions of EBV BOLF1 need to be elucidated.

In this study, we determined the functions of EBV BOLF1 by constructing knockout viruses using the EBV-BAC (Figs. 1–3) and CRISPR/Cas9 systems (Fig. 4). Recombinant EBV-BAC viruses, derived from the B95-8 strain, were evaluated in HEK293 cells, while the Akata strain EBV was edited using the CRISPR/Cas9 system and evaluated in Akata cells. Under both conditions, disrupting BOLF1 resulted in reduced progeny infectivity by approximately one order of magnitude, whereas viral protein expression, DNA synthesis, and extracellular progeny secretion were not affected (Figs. 1–4). We then investigated if progeny attachment was affected by knocking out BOLF1, but the rates of viral attachment to Akata(−) cells did not differ between knockout and wild-type viruses (both EBV-BAC (B95-8) and Akata strains) (Figs. 2E, 4E). Nuclear transportation of the incoming nucleocapsids was decreased by the disruption of BOLF1 gene (Tables 1 and 2). Therefore, inhibition of infectivity likely occurs at some point between viral entry and nuclear transportation. Similarly, a recent study on MuHV-4 ORF63 reported that ORF63-deficiency did not affect extracellular virion release but significantly impaired viral capsid migration towards the nucleus during viral entry (Latif et al., 2015). As the transportation of the incoming capsid of gammaherpesviruses rely on the microtubule network (Naranatt et al., 2005; Zhang et al., 2012), we hypothesize that after entry, BOLF1 mediates the interaction between viral capsid and microtubule motor proteins and facilitates capsid movement towards the nucleus. Further experiments are needed to confirm this hypothesis, but the analysis of nuclear transportation is challenging as EBV infection is not efficient even with wild-type viruses.

In HSV-1 and HCMV, the homologs of EBV BOLF1 (UL37 and UL47, respectively) are involved not only in the nuclear transportation of incoming nucleocapsids but also in secondary envelopment and egress (Bechtel and Shenk, 2002; McElwee et al., 2013; Pasdeloup et al., 2013). We were unable to determine why the disruption of EBV BOLF1 affected only the processes that occur after the virus binds to new cells, because the monitoring of processes such as secondary envelopment and egress of recombinant EBV is very difficult. Indeed, the

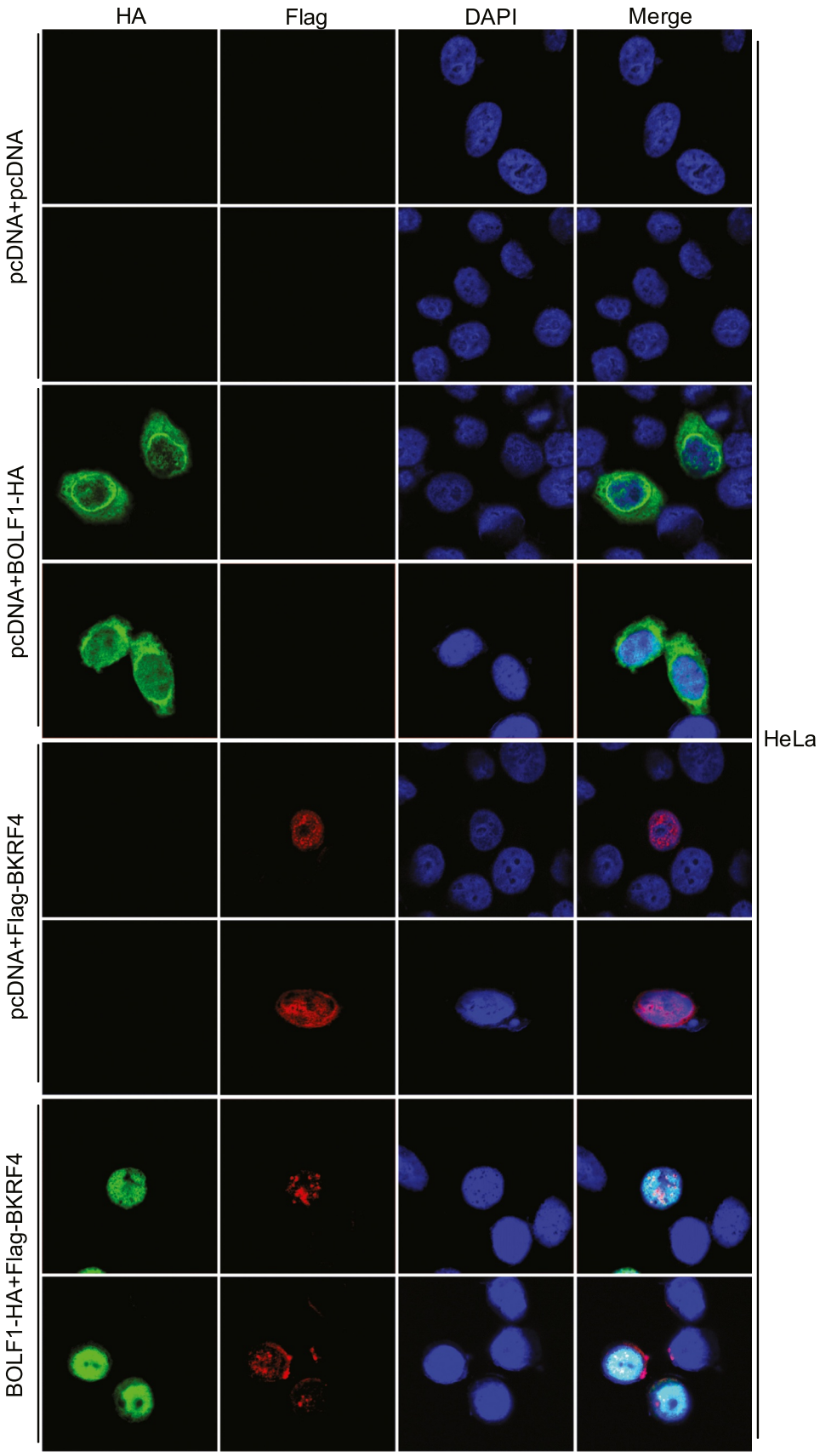

Fig. 6. BOLF1 was localized in both the nucleus and cytoplasm of BOLF1-transfected cells but was limited to the nucleus in cells co-transfected with BOLF1 and BKRF4. HeLa cells were transfected with expression vectors using lipofectamine. Cells were fixed at 1 day after transfection and stained with anti-Flag (red) and anti-HA (green) antibodies and DAPI. Samples were then examined by confocal laser microscopy.

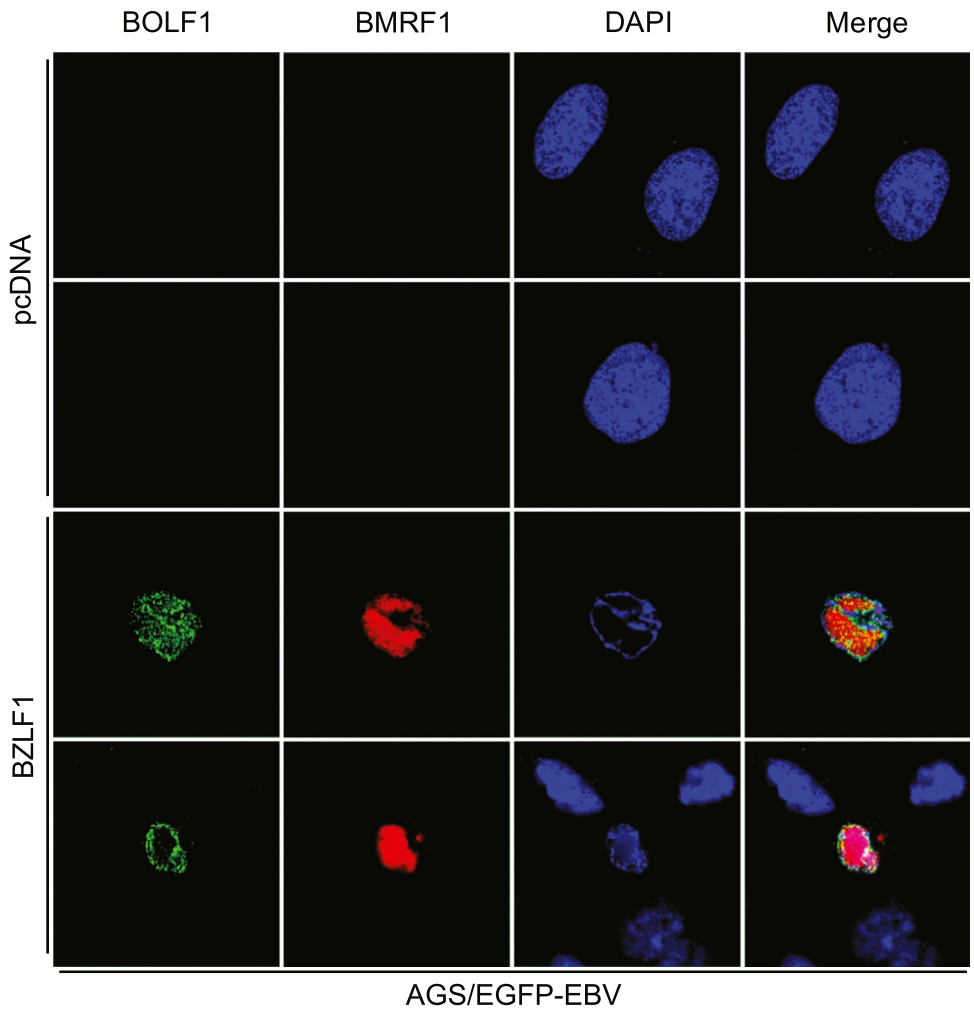

Fig. 7. Endogenous BOLF1 was localized in the nucleus and peri-nuclear region in AGS cells. The lytic cycle of AGS/EGFP–EBV cells was induced by transfection of the BZLF1 expression vector using lipofectamine. After 2 days, cells were fixed and stained with anti-BOLF1 (green) and anti-BMRF1 (red) antibodies and DAPI (blue) and then examined by confocal laser microscopy.

physiological roles of several EBV genes hypothesized to function in those processes, including BGLF3.5 (Watanabe et al., 2015a) and BSRF1 (manuscript in prep.), could not be observed.

From our immunoprecipitation assay, we found that EBV BOLF1 interacted with another EBV tegument protein, BKRF4 (Fig. 5). BOLF1 was localized in both the nucleus and cytoplasm when exogenously over-expressed without BKRF4 but was restricted to the nucleus when co-expressed with BKRF4 (Fig. 6). We also found that BOLF1 was localized in the nucleus and nuclear rim of infected AGS and Akata cells under lytic cycle, and that BOLF1 protein partially merged with BKRF4 protein in the nucleus (Figs. 7, 8A). So, we first speculated that nuclear dominant localization of BOLF1 was dependent of BKRF4, but the situation was different in infected cells; the BOLF1 protein still exhibited predominant nuclear localization even in the absence of BKRF4 (Fig. 8B). Therefore, BKRF4 can interact with BOLF1, and the BKRF4 can alter the localization to the nucleus under some specific over-expression conditions, but other viral factor can substitute in place of BKRF4 in the condition of lytic infection. Anyway, as BKRF4-deficiency resulted in reduced progeny viral production and infectivity (Masud et al., 2017), the interaction between BOLF1 and BKRF4 may contribute to the reduced infectivity of the BOLF1-deficient virus.

BKRF4 interacts with another tegument protein, BGLF2 (Konishi et al., 2018), in addition to the BOLF1 protein (Fig. 5). Because BGLF2 activates the AP-1/MAPK signaling pathway when it is released from the virion by de-envelopment, and increases viral gene expression and infectivity (Konishi et al., 2018), BGLF2 may also be involved in the reduced infectivity of the BOLF1-knockout strain.

In summary, this study demonstrated that EBV BOLF1 is required for efficient *de novo* infectivity. Despite having limited sequence conservation with homologs in other herpesviruses, BOLF1 still share some common functions with its homologs, particularly nuclear transportation of incoming nucleocapsids. Further analysis is required to clarify BOLF1 function.

4. Materials and methods

4.1. Cell culture and reagents

The cell lines HeLa, HEK293, HEK293 EBV-BAC, and HEK293T were cultured in a Dulbecco's Modified Eagle Medium (Sigma-Aldrich) supplemented with 10% fetal bovine serum (FBS). AGS/EGFP–EBV cells containing the recombinant Akata virus harboring EGFP and G418 resistance genes (Katsumura et al., 2009), and Akata(−) cells were cultured in RPMI 1640 (Sigma-Aldrich) medium containing 10% FBS.

The EBV BOLF1 antiserum was obtained by affinity purification using the synthetic peptide NH2-DIDTAARAQKVETSC-COOH, after immunizing a rabbit with the same peptide. The antibodies against BZLF1, BRLF1, BMRF1, BALF2, BGLF4, BALF4(gB), BALF5, BRRF2, BKRF4, and EBNA1 have been described previously (Asai et al., 2006; Daikoku et al., 2005; Masud et al., 2017; Murata et al., 2009; Watanabe

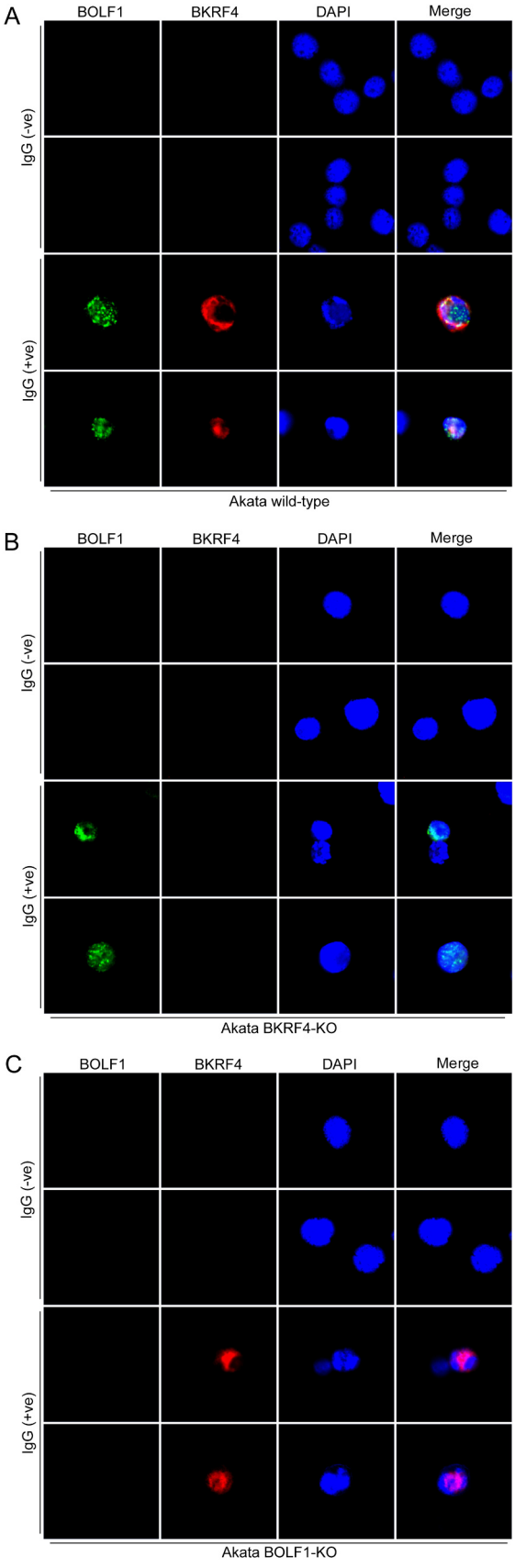

Fig. 8. Localization of BOLF1 and BKRF4 in Akata cells, and the effect of knockout of BOLF1 or BKRF4. (A-C) Akata wild-type (Fig. 8A), BKRF4-KO (Fig. 8B), and BOLF1-KO (Fig. 8C) cells were lytically induced by anti-IgG. After 2 days of induction, cells were fixed and stained with anti-BOLF1 (green) and anti-BKRF4 (red) antibodies and DAPI (blue) and then examined by confocal laser microscopy.

et al., 2015b). Mouse anti-Flag, mouse anti-BMRF1, anti-α/β-tubulin, and anti-HA antibodies were purchased from Sigma-Aldrich, Novocastra, Cell Signaling, and Roche. Horseradish peroxidase-conjugated secondary mouse and rabbit IgG antibodies were purchased from Amersham Biosciences. The Alexa 488- and Alexa 546-conjugated goat anti-rabbit and anti-mouse IgG secondary antibodies and the Zenon mouse IgG labeling kit were purchased from Molecular Probes.

4.2. Plasmids

The BZLF1, Flag-tagged BKRF4, and HA-tagged BOLF1 expression plasmids have been described previously (Konishi et al., 2018; Masud et al., 2017; Murata et al., 2009). To insert a stop codon into the BOLF1 sequence, the HA-tagged BOLF1 vector was used as a template and mutated by inverse PCR using the following primers: forward 5′-AGG ACTGGGGGATTTGGCCCA-3′ and reverse 5′-TAGATCCCCAGCTCCAG AGGC-3′.

To construct pX459-BOLF1, the vector used for CRISPR/Cas9-mediated BOLF1-knockout and two oligonucleotide sequences (forward 5′-CACCGATCTTTGGACTGGGGGATT-3′ and reverse 5′-AAACAATCCC CCAGTCCAAAGATC-3′) were annealed and inserted into the *Bbs*I site of pX459 (Addgene).

4.3. Genetic manipulation of the EBV-BAC genome and transfection into HEK293 cells

The B95-8 EBV-BAC DNA sequence was obtained from W. Hammerschmidt (Delecluse et al., 1998). To modify the EBV-BAC genome, homologous recombination was carried out in *Escherichia coli* as described in Murata et al. (2009).

The Neo/St marker cassette, which contains genes for neomycin resistance and streptomycin sensitivity, was used as the selection marker. Transfer DNA fragments for the first recombination event were generated by PCR using the rpsL-neo vector (Gene Bridges, Germany) as the template and the following primers: Neo/St forward 5′-TGTCTGG GGACGACCCCGCTGCCCGCCTGCGCGCGCTGATGCCTCTGGAGCTGGG GATCTGGCCTGGTGATGATGGCGGGATC-3′ and Neo/St reverse 5′-GAGGGTGAGAGTATTTAAAAAATCGCGCACCAGCACCGGCTGGGCC AAATCCCCCAGTCCTCAGAAGAACTCGTCAAGAAGG-3′. The intermediate insertion mutant was obtained by selection of kanamycin-resistant colonies after recombination and confirmed by colony PCR using the following primers: forward 5′-CTATGGAGAGTGACAGCAGC-3′ and reverse 5′-AAGCTGCGCCTGGAAAAGGA-3′. The dBOLF1-stop mutant was constructed by replacing the Neo/St cassette in the intermediate mutant with the BOLF1 sequence containing a stop codon. Colonies that contained the dBOLF1-stop EBV-BAC were selected using streptomycin. Finally, to prepare the revertant virus (dBOLF1-stop/R), the Neo/St cassette was again inserted to make the intermediate, and then replaced by wild-type BOLF1.

Electroporation was conducted using the Gene Pulser III (Bio-Rad), and EBV-BAC DNA was purified using the NucleoBond Bac100 (Macherey–Nagel). Recombination was confirmed by PCR, sequence analysis, and agarose gel electrophoresis of the *Bam*HI- or *Eco*RI-digested viral genome.

To generate the cell clones, HEK293 cells were transfected with the recombinant EBV-BAC DNA using Lipofectamine 2000 reagent (Invitrogen). GFP-positive and hygromycin-resistant cell colonies were selected for use in further analyses.

4.4. BOLF1 knockout preparation using the CRISPR/cas9 system

BOLF1-deficient Akata virus was prepared according to Masud et al. (2017). Briefly, AGS/EGFP–EBV cells containing recombinant Akata virus were transfected with pX459-BOLF1 by lipofection. After puromycin selection, BZLF1 was transfected by electroporation to induce progeny production, and cell-free supernatants containing viral particles were then collected and used to infect Akata(−) cells. GFP-positive cell clones were prepared by selection with 750 μg/ml G418, after limiting dilution and cloning for 3–4 weeks.

4.5. Immunoblotting

HEK293 cells harboring the latent EBV genome were transfected with the BZLF1 expression vector by electroporation (Neon Transfection System, Thermo Fisher Scientific) to induce lytic replication. Two days after transfection, cells were washed with PBS and harvested, and cell lysates were subjected to immunoblotting as described in Murata et al. (2009). Lytic induction of the EBVs in Akata cells was conducted by adding anti-IgG antibody for 2 days.

4.6. Quantification of the level of EBV DNA synthesis by qPCR

Levels of viral DNA synthesis were quantified by qPCR using the Fast Start Universal Probe Master (Rox; Roche Applied Science) according to Narita et al. (2013). Cells were washed with PBS and then lysed in lysis buffer containing proteinase K with sonication, followed by proteinase K deactivation. A standard curve prepared with serial dilutions of DNA was used to quantify the DNA. Primers and a probe targeting the BALF2-coding region were designed to detect the EBV genome.

4.7. Determination of viral titers using FACS

The latent EBV genome in HEK293 cells was lytically induced by BZLF1 transfection using the Neon transfection system. Three days after transfection, culture media were collected, centrifuged, and filtered. In Akata cell clones, the genome was lytically induced using anti-IgG antibody for 2 days, followed by centrifugation and filtration.

Next, Akata(−) cells were co-cultured with the virus-containing supernatants for 3 h at room temperature with rotation. After low-speed centrifugation, the resulting cell pellets were resuspended in fresh medium and cultured for 2 days. Cells were then fixed in 1% formaldehyde, rinsed with PBS, and resuspended in PBS. The percentage of GFP-positive cells was calculated using the FACSCalibur G5 system (Becton Dickinson).

4.8. Quantification of extracellular EBV virion DNA

Extracellular virion DNA was quantified by qPCR as described in Wang et al. (2015), with some modifications (Masud et al., 2017). Briefly, 200 μl virus stock were treated with 2 μl Turbo DNase I (Thermo Fisher Scientific), and the reaction was stopped by adding EDTA, followed by heat inactivation of DNase I at 75 °C for 10 min. DNA was extracted using the DNeasy blood and tissue kit (Qiagen), and viral DNA levels were quantified as described above.

4.9. Quantification of viral DNA bound to the host cells and transported to the nucleus

Viral DNAs bound to the host cells were quantified by qPCR as described previously (Masud et al., 2017). Briefly, Akata(−) cells were incubated with virus stock solutions for 3 h at 4 °C with rotation and washed with PBS 3–4 times. Samples were then treated with Turbo DNase I followed by the inactivation of DNase I using inactivation reagent (Thermo Fisher Scientific) and the cell-associated DNA was extracted and quantified as described above.

For nuclear transportation assay, after virus attachment of virus particles for 3 h at 4 °C with rotation, cells were treated with and inactivated DNase I. The cells were then incubated at 37 °C for 6 h, followed by nuclear fractionation using EzSubcell Fraction kit (ATTO) according to the manufacturer's instruction. Finally, EBV DNAs associated with nuclei were extracted and quantified as described above.

4.10. Immunoprecipitation

HEK293T cells were transfected with indicated plasmid vectors using Lipofectamine 2000 reagent. After 24 h, cells were solubilized in immunoprecipitation lysis buffer (20 mM Tris-HCl at pH 7.8, 200 mM NaCl, 0.5% Nonidet P-40, 1 mM EDTA, 0.5% Triton X, and protease inhibitor cocktail tablets [Complete mini, Roche]), followed by sonication and centrifugation at 15,000 rpm for 5 min. Anti-HA/Anti-FLAG mouse antibodies and G-Sepharose 4 Fast Flow (GE Healthcare) were then added to the supernatants and rotated at 4 °C for more than 2 h. Next, the immunocomplexes were washed extensively (four or five times) with the same immunoprecipitation lysis buffer and subjected to immunoblotting using the respective antibodies.

4.11. Immunofluorescence analysis and confocal microscopy

Immunofluorescence analysis was conducted as described in Masud et al. (2017). HeLa cells were first transfected with specific vectors. The next day, cells were fixed, permeabilized, blocked, and incubated with the primary antibodies. Then, cells were washed with PBS, treated with secondary antibodies, and washed again with PBS. Finally, cell samples were mounted in the ProLong Gold antifade reagent with DAPI (Molecular Probes).

AGS/EGFP–EBV cells containing the recombinant Akata virus were transfected with BZLF1 for 2 days using Lipofectamine 2000 reagent to induce lytic induction. The cells were then processed as described above, incubated with anti-BOLF1 rabbit and anti-BMRF1 mouse antibodies, and stained with secondary antibodies (Alexa 488 anti-rabbit IgG and Alexa 546 anti-mouse IgG; Invitrogen).

For Akata cells, since both of the BOLF1 and BKRF4 antibodies were rabbit-derived, anti-BKRF4 antibody was directly crosslinked with fluorescence dye by using Zenon Alexa Fluor 555 rabbit IgG labeling kit according to the manufacturer's instruction. Akata cells were lytically induced using anti-IgG for 2 days, and the samples were incubated with anti-BOLF1 rabbit antibody, followed by secondary staining with Alexa 488 anti-rabbit IgG antibody (Invitrogen). Then, after the samples were blocked once again, and treated with Alexa Fluor 555-labelled anti-BKRF4 antibody.

Samples were examined using the LSM880 confocal microscope (Zeiss).

Acknowledgements

We thank Drs. W. Hammerschmidt, H. J. Delecluse, T. Kanda, and T. Tsurumi for materials and discussions. This work was supported by grants-in-aid for Scientific Research from the Ministry of Education, Culture, Sports, Science and Technology (to T.M. (15K08494) and H.K. (17H04081)), Japan Agency for Medical Research and Development (to T.M. (Japanese Initiative for Progress of Research on Infectious Disease for Global Epidemic, JP17fm0208016) and H.K. (Practical Research Project for Rare/Intractable Diseases, JP16ek0109098)), the Takeda Science Foundation (to T.M.), and the Hori Sciences and Arts Foundation (to T.M. and H.K.).

References

Asai, R., Kato, A., Kato, K., Kanamori-Koyama, M., Sugimoto, K., Sairenji, T., Nishiyama, Y., Kawaguchi, Y., 2006. Epstein-Barr virus protein kinase BGLF4 is a virion tegument

protein that dissociates from virions in a phosphorylation-dependent process and phosphorylates the viral immediate-early protein BZLF1. J. Virol. 80, 5125–5134.
Bechtel, J.T., Shenk, T., 2002. Human cytomegalovirus UL47 tegument protein functions after entry and before immediate-early gene expression. J. Virol. 76, 1043–1050.
Cappadona, I., Villinger, C., Schutzius, G., Mertens, T., von Einem, J., 2015. Human cytomegalovirus pUL47 modulates tegumentation and capsid accumulation at the viral assembly complex. J. Virol. 89, 7314–7328.
Cardone, G., Newcomb, W.W., Cheng, N., Wingfield, P.T., Trus, B.L., Brown, J.C., Steven, A.C., 2012. The UL36 tegument protein of herpes simplex virus 1 has a composite binding site at the capsid vertices. J. Virol. 86, 4058–4064.
Daikoku, T., Kudoh, A., Fujita, M., Sugaya, Y., Isomura, H., Shirata, N., Tsurumi, T., 2005. Architecture of replication compartments formed during Epstein-Barr virus lytic replication. J. Virol. 79, 3409–3418.
Delecluse, H.J., Hilsendegen, T., Pich, D., Zeidler, R., Hammerschmidt, W., 1998. Propagation and recovery of intact, infectious Epstein-Barr virus from prokaryotic to human cells. Proc. Natl. Acad. Sci. USA 95, 8245–8250.
Desai, P., Sexton, G.L., Huang, E., Person, S., 2008. Localization of herpes simplex virus type 1 UL37 in the Golgi complex requires UL36 but not capsid structures. J. Virol. 82, 11354–11361.
Desai, P., Sexton, G.L., McCaffery, J.M., Person, S., 2001. A null mutation in the gene encoding the herpes simplex virus type 1 UL37 polypeptide abrogates virus maturation. J. Virol. 75, 10259–10271.
Diefenbach, R.J., 2015. Conserved tegument protein complexes: essential components in the assembly of herpesviruses. Virus Res 210, 308–317.
Gregory, S.M., Davis, B.K., West, J.A., Taxman, D.J., Matsuzawa, S., Reed, J.C., Ting, J.P., Damania, B., 2011. Discovery of a viral NLR homolog that inhibits the inflammasome. Science 331, 330–334.
Hammerschmidt, W., Sugden, B., 2013. Replication of Epstein-Barr viral DNA. Cold Spring Harb. Perspect. Biol. 5, a013029.
Johannsen, E., Luftig, M., Chase, M.R., Weicksel, S., Cahir-McFarland, E., Illanes, D., Sarracino, D., Kieff, E., 2004. Proteins of purified Epstein-Barr virus. Proc. Natl. Acad. Sci. USA 101, 16286–16291.
Katsumura, K.R., Maruo, S., Wu, Y., Kanda, T., Takada, K., 2009. Quantitative evaluation of the role of Epstein-Barr virus immediate-early protein BZLF1 in B-cell transformation. J. Gen. Virol. 90, 2331–2341.
Kelly, B.J., Bauerfeind, R., Binz, A., Sodeik, B., Laimbacher, A.S., Fraefel, C., Diefenbach, R.J., 2014. The interaction of the HSV-1 tegument proteins pUL36 and pUL37 is essential for secondary envelopment during viral egress. Virology 454–455, 67–77.
Klupp, B.G., Fuchs, W., Granzow, H., Nixdorf, R., Mettenleiter, T.C., 2002. Pseudorabies virus UL36 tegument protein physically interacts with the UL37 protein. J. Virol. 76, 3065–3071.
Klupp, B.G., Granzow, H., Mundt, E., Mettenleiter, T.C., 2001. Pseudorabies virus UL37 gene product is involved in secondary envelopment. J. Virol. 75, 8927–8936.
Konishi, N., Narita, Y., Hijioka, F., Masud, H., Sato, Y., Kimura, H., Murata, T., 2018. BGLF2 increases infectivity of Epstein-Barr Virus by activating AP-1 upon De Novo infection. mSphere 3 (e00138-18).
Latif, M.B., Machiels, B., Xiao, X., Mast, J., Vanderplasschen, A., Gillet, L., 2015. Deletion of Murid Herpesvirus 4 ORF63 affects the trafficking of incoming capsids toward the nucleus. J. Virol. 90, 2455–2472.
Leege, T., Granzow, H., Fuchs, W., Klupp, B.G., Mettenleiter, T.C., 2009. Phenotypic similarities and differences between UL37-deleted pseudorabies virus and herpes simplex virus type 1. J. Gen. Virol. 90, 1560–1568.
Lieberman, P.M., 2015. Chromatin structure of Epstein-Barr Virus latent episomes. Curr. Top. Microbiol. Immunol. 390, 71–102.
Masud, H., Watanabe, T., Yoshida, M., Sato, Y., Goshima, F., Kimura, H., Murata, T., 2017. Epstein-Barr Virus BKRF4 gene product is required for efficient progeny production. J. Virol. 91.
McElwee, M., Beilstein, F., Labetoulle, M., Rixon, F.J., Pasdeloup, D., 2013. Dystonin/BPAG1 promotes plus-end-directed transport of herpes simplex virus 1 capsids on microtubules during entry. J. Virol. 87, 11008–11018.
Murata, T., 2014. Regulation of Epstein-Barr virus reactivation from latency. Microbiol Immunol. 58, 307–317.
Murata, T., 2018. Encyclopedia of EBV-Encoded lytic genes: an update. Adv. Exp. Med. Biol. 1045, 395–412.
Murata, T., Isomura, H., Yamashita, Y., Toyama, S., Sato, Y., Nakayama, S., Kudoh, A., Iwahori, S., Kanda, T., Tsurumi, T., 2009. Efficient production of infectious viruses requires enzymatic activity of Epstein-Barr virus protein kinase. Virology 389, 75–81.
Murata, T., Sato, Y., Kimura, H., 2014. Modes of infection and oncogenesis by the Epstein-Barr virus. Rev. Med. Virol. 24, 242–253.
Murata, T., Tsurumi, T., 2014. Switching of EBV cycles between latent and lytic states. Rev. Med. Virol. 24, 142–153.
Naranatt, P.P., Krishnan, H.H., Smith, M.S., Chandran, B., 2005. Kaposi's sarcoma-associated herpesvirus modulates microtubule dynamics via RhoA-GTP-diaphanous 2 signaling and utilizes the dynein motors to deliver its DNA to the nucleus. J. Virol. 79, 1191–1206.
Narita, Y., Murata, T., Ryo, A., Kawashima, D., Sugimoto, A., Kanda, T., Kimura, H., Tsurumi, T., 2013. Pin1 interacts with the Epstein-Barr virus DNA polymerase catalytic subunit and regulates viral DNA replication. J. Virol. 87, 2120–2127.
Owen, D.J., Crump, C.M., Graham, S.C., 2015. Tegument assembly and secondary envelopment of Alphaherpesviruses. Viruses 7, 5084–5114.
Pasdeloup, D., McElwee, M., Beilstein, F., Labetoulle, M., Rixon, F.J., 2013. Herpesvirus tegument protein pUL37 interacts with dystonin/BPAG1 to promote capsid transport on microtubules during egress. J. Virol. 87, 2857–2867.
Richards, A.L., Sollars, P.J., Pitts, J.D., Stults, A.M., Heldwein, E.E., Pickard, G.E., Smith, G.A., 2017. The pUL37 tegument protein guides alpha-herpesvirus retrograde axonal transport to promote neuroinvasion. PLoS Pathog. 13, e1006741.
Rozen, R., Sathish, N., Li, Y., Yuan, Y., 2008. Virion-wide protein interactions of Kaposi's sarcoma-associated herpesvirus. J. Virol. 82, 4742–4750.
Russo, J.J., Bohenzky, R.A., Chien, M.C., Chen, J., Yan, M., Maddalena, D., Parry, J.P., Peruzzi, D., Edelman, I.S., Chang, Y., Moore, P.S., 1996. Nucleotide sequence of the Kaposi sarcoma-associated herpesvirus (HHV8). Proc. Natl. Acad. Sci. USA 93, 14862–14867.
Sathish, N., Wang, X., Yuan, Y., 2012. Tegument proteins of Kaposi's Sarcoma-associated Herpesvirus and related Gamma-Herpesviruses. Front. Microbiol. 3, 98.
Song, M.J., Hwang, S., Wong, W.H., Wu, T.T., Lee, S., Liao, H.I., Sun, R., 2005. Identification of viral genes essential for replication of murine gamma-herpesvirus 68 using signature-tagged mutagenesis. Proc. Natl. Acad. Sci. USA 102, 3805–3810.
Tullman, J.A., Harmon, M.E., Delannoy, M., Gibson, W., 2014. Recovery of an HMWP/hmwBP (pUL48/pUL47) complex from virions of human cytomegalovirus: subunit interactions, oligomer composition, and deubiquitylase activity. J. Virol. 88, 8256–8267.
Vittone, V., Diefenbach, E., Triffett, D., Douglas, M.W., Cunningham, A.L., Diefenbach, R.J., 2005. Determination of interactions between tegument proteins of herpes simplex virus type 1. J. Virol. 79, 9566–9571.
Wang, X., Zhu, N., Li, W., Zhu, F., Wang, Y., Yuan, Y., 2015. Mono-ubiquitylated ORF45 mediates association of KSHV particles with internal lipid rafts for viral assembly and egress. PLoS Pathog. 11, e1005332.
Watanabe, T., Fuse, K., Takano, T., Narita, Y., Goshima, F., Kimura, H., Murata, T., 2015a. Roles of Epstein-Barr virus BGLF3.5 gene and two upstream open reading frames in lytic viral replication in HEK293 cells. Virology 483, 44–53.
Watanabe, T., Tsuruoka, M., Narita, Y., Katsuya, R., Goshima, F., Kimura, H., Murata, T., 2015b. The Epstein-Barr virus BRRF2 gene product is involved in viral progeny production. Virology 484, 33–40.
Young, L.S., Rickinson, A.B., 2004. Epstein-Barr virus: 40 years on. Nat. Rev. Cancer 4, 757–768.
Zhang, J., Zhao, J., Xu, S., Li, J., He, S., Zeng, Y., Xie, L., Xie, N., Liu, T., Lee, K., Seo, G.J., Chen, L., Stabell, A.C., Xia, Z., Sawyer, S.L., Jung, J., Huang, C., Feng, P., 2018. Species-specific deamidation of cGAS by Herpes Simplex Virus UL37 protein facilitates viral replication. Cell Host Microbe 24, 234–248 (e235).
Zhang, W., Greene, W., Gao, S.J., 2012. Microtubule- and dynein-dependent nuclear trafficking of rhesus rhadinovirus in rhesus fibroblasts. J. Virol. 86, 599–604.